

## Coexistence of magnetism and superconductivity in $R_{1.4}\text{Ce}_{0.6}\text{RuSr}_2\text{Cu}_2\text{O}_{10-\delta}$ ( $R=\text{Eu}$ and $\text{Gd}$ )

I. Felner, U. Asaf, Y. Levi, and O. Millo

*Racah Institute of Physics, The Hebrew University, Jerusalem, 91904, Israel*

(Received 16 September 1996)

The superconducting  $R_{1.4}\text{Ce}_{0.6}\text{RuSr}_2\text{Cu}_2\text{O}_{10-\delta}$  materials are also magnetically ordered at  $T_N \gg T_c$  ( $T_c \sim 42, 32$  and  $T_N \sim 180, 122$  K for  $R=\text{Gd}$  and  $\text{Eu}$ , respectively). Magnetic susceptibility and Mössbauer spectroscopy show that superconductivity is confined to the  $\text{CuO}_2$  planes, whereas magnetism is due to the Ru sublattice. Scanning-tunneling-spectroscopy measurements reveal a superconducting gap structure for the whole sample, indicating that the materials are of single phase, which simultaneously manifest both superconductivity and magnetism. [S0163-1829(97)50706-5]

Superconductivity (SC) and magnetism are two different ordered states into which substances can condense at low temperatures and in general these states are inimical to one another. In conventional  $s$ -wave superconductors, local magnetic moments break up the spin singlet Cooper pairs and hence strongly suppress SC, an effect known as pair breaking. Therefore, a level of magnetic impurity of only 1% can result in a complete loss of SC. In a limited class of intermetallic systems, SC occurs even though magnetic ions with a local moment occupy all of one specific crystallographic site, which is well isolated and decoupled from the conduction path. The study of this class of magnetic superconductors was initiated by the discovery of  $\text{RRh}_4\text{B}_4$  and  $\text{RMo}_6\text{S}_8$  compounds ( $R=\text{rare-earth}$ ),<sup>1</sup> and has been recently revitalized by the discovery of the  $\text{RNi}_2\text{B}_2\text{C}$  system.<sup>2</sup> In all three systems, both SC and antiferromagnetic (AFM) order states coexist. The onset of SC takes place at relatively high temperatures ( $T_c \sim 2\text{--}15$  K), while AFM order appears at lower temperatures (except for  $\text{DyNi}_2\text{B}_2\text{C}$ ), and the typical ratio  $T_N/T_c$  is about 0.1–0.5. Despite progress in understanding both states in the intermetallic systems, there has been no evidence to date for a magnetic superconductor in the Cu-O based high- $T_c$  superconducting compounds (HTSC's). In fact, many of the HTSC systems contain magnetic  $R$  ions as structural constituents, which are electronically isolated from the Cu-O planes, and have no adverse effect upon the superconducting state. However, the  $T_N(R)$  values are quite low; e.g., in  $\text{RBa}_2\text{Cu}_3\text{O}_7$  (RBCO) with  $T_c \sim 92$  K, regardless of  $R$ , the highest  $T_N$  obtained is 2.2 K, for  $R=\text{Gd}$ .

Much attention has been focused on a phase resembling the RBCO materials, having the composition  $R_{1.5}\text{Ce}_{0.5}\text{MSr}_2\text{Cu}_2\text{O}_{10}$  ( $M=2122$ ,  $M=\text{Nb}$ ,  $\text{Ru}$ , or  $\text{Ta}$ ).<sup>3–5</sup> The tetragonal  $M$ -2122 structure evolves from the RBCO structure by inserting a fluorite type  $R_{1.5}\text{Ce}_{0.5}\text{O}_2$  layer instead of the  $R$  layer in RBCO, thus shifting alternate perovskite blocks by  $(a+b)/2$ . The  $M$  ions reside in the Cu(1) site and only one distinct Cu site [corresponding to Cu(2) in RBCO] with fivefold pyramidal coordination exists. The hole doping of the Cu-O planes, which results in metallic behavior and SC, can be optimized with appropriate variation of the  $[R]/[\text{Ce}]$  ratio. Nb-2122 and Ru-2122 systems are SC with  $T_c \sim 28$  and 42 K.<sup>3,6</sup> Here we present a study on a new magnetic superconductor in the ceramic HTSC materials, with a magnetic ordering well above the SC state ( $T_N/T_c \sim 4$ ), a trend which is contrary to that observed in the intermetallic systems. We demonstrate that  $R_{1.4}\text{Ce}_{0.6}\text{RuSr}_2\text{Cu}_2\text{O}_{10-\delta}$

( $\text{RCeRuSCO}$ ,  $R=\text{Eu}$  and  $\text{Gd}$ ) compounds exhibit coexistence of bulk SC ( $T_c=32, 42$  K) in the magnetic state ( $T_N=122, 180$  K) for  $R=\text{Gd}$  and  $\text{Eu}$ , respectively. In addition, our Mössbauer spectroscopy studies (MS) on  $^{57}\text{Fe}$ -doped samples clearly indicate that the magnetic state is confined to the Ru site. Scanning tunneling microscopy (STM) data, in particular spatially resolved tunneling  $I$ - $V$  characteristics, suggest that the samples are of single phase, and do not consist of mixed normal (magnetic) and superconducting phases.

$\text{RCeRuSCO}$  (and the 0.5 at. %  $^{57}\text{Fe}$ -doped) ceramic samples were prepared by a solid-state reaction and studied by ac and dc magnetic susceptibility and MS techniques, as described in our previous paper.<sup>5</sup> X-ray diffraction measurements indicate that the materials are nearly single phase ( $\sim 98\%$ ) and have the tetragonal structure ( $I4/mmm$ ) with  $a=3.846(1), 3.844(1)$ , and  $c=28.50(1), 28.62(1)$  Å for  $R=\text{Eu}$  and  $\text{Gd}$ , respectively. Specimens for STM measurements were mechanically polished with  $0.25\mu$  diamond lapping compound and then reannealed in oxygen for 15 h, just before mounting onto the cryogenic STM.

The temperature dependence of the normalized resistivity for  $\text{GdCeRuSCO}$  measured at  $H=0$  T is shown in Fig. 1(c) (inset). At high temperatures, a metallic behavior is observed, and the  $T_c=42$  K obtained is in agreement with Ref. 6. An applied field of 5 T smears the onset of SC and shifts it to 39 K. In  $\text{GdCeRuSCO}$ , SC occurs for Ce contents of 0.5–0.7, where the highest  $T_c$  was obtained for Ce=0.6, the concentration which has been studied here. Generally speaking, the magnetization in these samples is composed of three contributions: (a) a negative moment below  $T_c$  due to the SC state, (b) a positive moment due to the paramagnetic effective moment of  $R$  ( $P_{\text{eff}}=7.94\mu_B$  for  $R=\text{Gd}$ ), and (c) a contribution from the ferromagneticlike behavior of the Ru sublattice. In addition, there may be a positive contribution to the magnetization, due to the fact that a small remanent field exists in our superconducting quantum interference device magnetometer. This artificial contribution will affect mainly the magnetization measured at low applied fields. Zero-field-cooled (ZFC) and field-cooled (FC) magnetic measurements were performed for a broad range of  $H$  strengths, and typical susceptibility  $[\chi(T)]$  curves are shown in Fig. 1. At  $H=5$  Oe, both ZFC and FC branches exhibit two magnetic anomalies at 102 K and at  $T_{\text{irr}}=172$  K [Fig. 1(a)].  $T_{\text{irr}}$  is defined as the merging temperature of the ZFC and FC branches (where the difference between the branches becomes less than

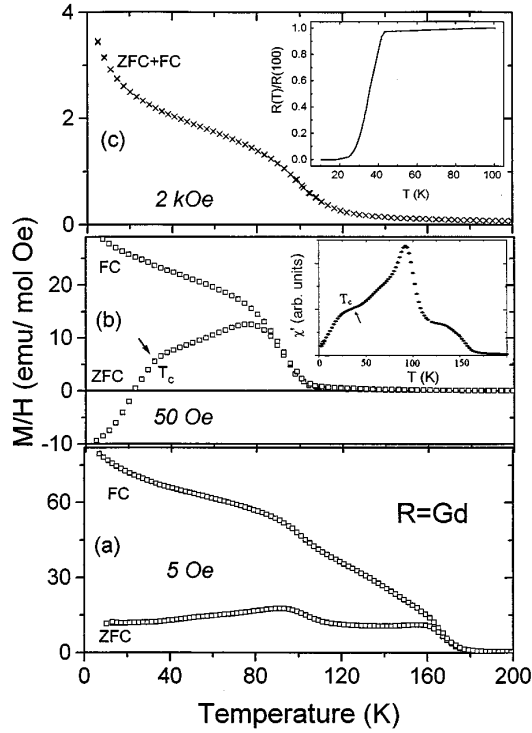


FIG. 1. ZFC and FC susceptibility curves for GdCeRuSCO measured at 5 and 50 Oe and at 2 kOe. Note the negative signal at  $H=50$  Oe. The insets show the normalized resistivity (c) and the ac susceptibility (b).

$\Delta\chi=1\times 10^{-2}$  emu/mol Oe). No other anomalies were observed at higher temperatures. Annealing in high oxygen pressure (50 atm) did not affect this magnetic behavior. Our ac susceptibility measurements (frequency 100 Hz at  $H=1$  Oe) show similar shape and comparable dimensions to the ZFC curve [Fig. 1(b) (inset)]. No sign for magnetic ordering of the Gd sublattice down to 1.5 K is observed, either in ac or in dc measurements. As we shall argue, SC is confined to the  $\text{CuO}_2$  planes; therefore, all the magnetic anomalies in Figs. 1 are related to the Ru-O planes. Note that  $T_N(\text{Ru})$  is not at  $T_{\text{irr}}$ . The  $\chi(T)$  curves in Fig. 1 do not lend themselves to an easy determination of  $T_N(\text{Ru})$ , because of the high susceptibility of the  $\text{Gd}^{3+}$  ions which mask this transition. For this purpose we adapted the MS technique, which clearly indicates that  $T_N(\text{Ru})=180(5)$  K. The irreversibility at  $T_{\text{irr}}$  arises as a result of an antisymmetric exchange coupling of the Dzyaloshinsky-Moriya (DM) type<sup>7</sup> between neighboring Ru moments, induced by a local distortion that breaks the tetragonal symmetry of the  $\text{RuO}_6$  octahedra. Due to this DM interaction, the field causes the spins to cant slightly out of their original direction and to align a component of the moments with the direction of  $H$ . At low temperatures, the Ru-Ru and/or Gd-Ru interactions begin to dominate, leading to reorientation of the Ru moments, and the peak at 102 K is observed. The exact nature of the local structural distortions causing this reorientation is not presently known. Note that the ZFC branch is not negative below  $T_c$ , due to the remanent field in our apparatus (discussed above), which induces a positive moment at  $T_{\text{irr}}$  during the ZFC process.

At 50 Oe the diamagnetic signal due to the high shielding fraction (SF) of the SC state dominates, and the net moment at low  $T$  is negative [Fig. 1(b)]. The weak ferromagnetic component of Ru and the high paramagnetic effective moment of  $\text{Gd}^{3+}$  do not permit a quantitative determination of

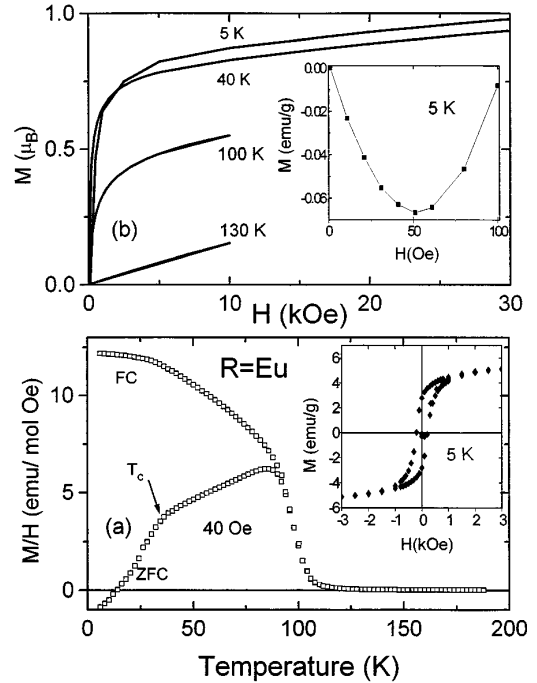


FIG. 2. (a) The ZFC and FC susceptibility for EuCeRuSCO at 40 Oe and (b) the isothermal magnetization as a function of the applied field. The insets show (a) the magnetic hysteresis loop and (b) the negative field dependence of the magnetization at 5 K at low applied fields.

the SF.  $T_c$  can also easily be determined from the deflection point in the ZFC curve. Both the temperatures at which reorientation occurs and  $T_{\text{irr}}$  are shifted to 80 and 112 K, respectively. This trend is easily understood by recognizing it as a typical characteristic of *weak*-ferromagnetic behavior. Isothermal magnetization measurements at various temperatures (not shown) indicate that the Ru moment saturates around 2 kOe; therefore, at this field both the anomalies and the irreversibility are washed out [Fig. 1(c)]. Similar magnetic behavior was observed in our  $^{57}\text{Fe}$ -doped sample prepared for a MS study, presented hereafter.

The magnetic behavior for EuCeRuSCO is shown in Fig. 2. At 40 Oe [Fig. 2(a)], the moment in the ZFC branch (below  $\sim 18$  K) is negative, and  $T_c=32$  K was deduced from this curve and from resistivity measurements.  $T_{\text{irr}}=92$  K, and no irreversibility phenomena are observed at 2 kOe.  $M(H)$  measurements at various temperatures have been performed, and due to the low susceptibility of  $\text{Eu}^{3+}$  ( $J=0$ ), both the magnetic and the SC states are clearly observed in the curves. At 5 K, (i) a small hysteresis loop is opened below 1.5 kOe [Fig. 2(b) (inset)], and (ii) the negative moments increase linearly up to 30 Oe [Fig. 2(a) (inset)], typical for a SC state below  $H_{c1}$ . The estimated SF deduced from this curve (ignoring possible contributions from Ru and/or  $\text{Eu}^{3+}$ ) is  $\sim 30\%$ , indicating bulk SC. Figure 2(b) shows that all  $M(H)$  curves below 130 K are strongly dependent on the field, up to about 1–2 kOe, until a common slope is reached.  $M(H)$  can be described as  $M(H)=\sigma_s+\chi H$ , where  $\chi H$  is the linear contribution of  $\text{Eu}^{3+}$  to the magnetization, and  $\sigma_s$ , which reaches its maximum at about 2 kOe, corresponds to the *weak*-ferromagnetic component of the Ru sublattice. At 5 K we obtained  $\sigma_s=0.83(3)\mu_B$  [defined as  $\sigma_s(0)$ ], a value which is much smaller than  $2\mu_B$  obtained for  $\text{Ru}^{4+}$  in  $\text{SrRuO}_3$ .  $\sigma_s$  decreases with increasing  $T$  and becomes zero at

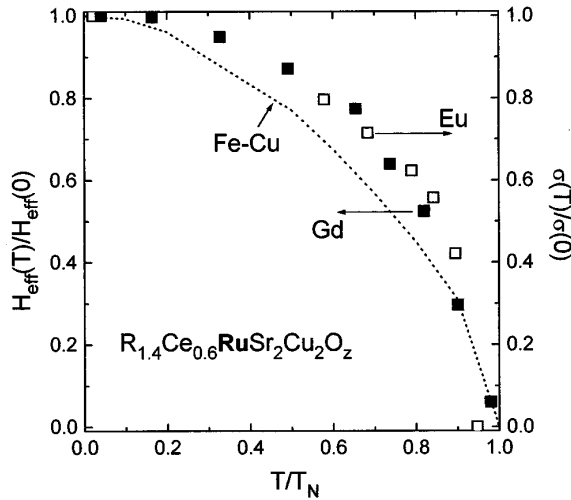


FIG. 3. The temperature dependence of (i) the normalized hyperfine field acting on Fe in the Ru sites for  $R=\text{Gd}$  (hollow squares, left scale) and (ii) the reduced magnetic moment of Ru deduced from magnetic measurements for  $R=\text{Eu}$  (right scale). The dashed line is the universal theoretical curve for Fe-Cu exchange strength. Note the deviation of the experimental data from the universal curve.

$T_N(\text{Ru})=122(1)$  K. The normalized  $\sigma_s(T)/\sigma_s(0)$  versus the reduced temperature ( $T/T_N$ ) are shown in Fig. 3, and will be discussed later. For  $R=\text{Gd}$ , the  $M(H)$  curve at 5 K is not linear at high  $H$  and therefore no easy determination of  $\sigma_s(0)$  can be made. Above  $T_N(\text{Ru})$ , the  $\chi(T)$  at 10 kOe for both samples adheres closely to the Curie-Weiss law. Note that in the  $RCeRuSCO$  system both  $T_c$  and  $T_N(\text{Ru})$  are higher for  $R=\text{Gd}$  than for  $R=\text{Eu}$ . In that respect it differs from similar  $M-2122$  ( $M=\text{Nb,Ta}$ ) systems in which  $T_c$  is the same for any  $R$  measured.<sup>8</sup> However, this is of little interest in the present discussion.

MS has been proved to be a powerful tool in the determination of the magnetic nature of the Fe site location. When the ions of this site become magnetically ordered, they produce an exchange field on the Fe ions residing in this site. The Fe nuclei experience a magnetic hyperfine field leading to a sextet in the observed MS spectra. As the temperature is raised, the magnetic splitting decreases and disappears at  $T_N$ . It is well accepted that in Y-Ba-Cu-O, the Fe atoms are found to occupy predominantly the Cu(1) site.<sup>9</sup>

The main effect to be seen in Fig. 4 is that the MS spectra of GdCeRuSCO consist of one site only, below and above  $T_N(\text{Ru})$ . A least-square fit to the spectrum at 180 K yields an isomer shift (IS) of 0.30(1) (relative to Fe metal) with a linewidth of 0.35, and a quadrupole splitting ( $\Delta_Q = \frac{1}{2}eQq$ ) of 1.00(1) mm/s values. We attribute this doublet to Fe ions in the Ru site. This interpretation is consistent with (i) the similarity of the chemical properties of Fe and Ru (Ru resides below Fe in the periodic table) and (ii) and with the fact that in most HTSC materials the Fe atoms are found to occupy predominantly the Cu(1) site, which is equivalent to the Ru site in the  $RCeRuSCO$ . At low temperatures, all spectra display magnetic hyperfine splitting, which is a clear evidence for long-range magnetic ordering. The fitting parameters of the single sextet obtained at 4.1 K are IS=0.40(1) mm/s,  $H_{\text{eff}}(0)=467(3)$  kOe, and an effective quadrupole splitting value of  $\Delta_{\text{eff}} = \frac{1}{2}eQq_{\text{eff}} = -0.33(21)$  mm/s. Using the relation  $\Delta_{\text{eff}} = \Delta_Q/2(3 \cos^2\Theta - 1)$ , we obtained for the Ru site a hy-

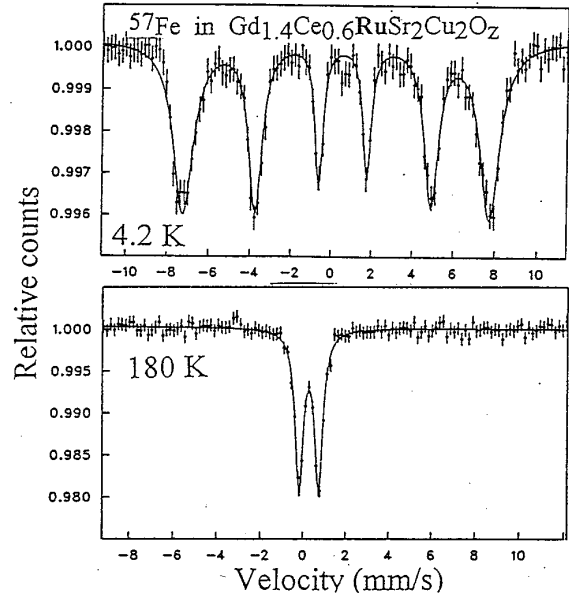


FIG. 4. Mössbauer spectra of 0.5%  $^{57}\text{Fe}$  doped in GdCeRuSCO below and above  $T_N(\text{Ru})$ .

perfine field orientation,  $\Theta=72^\circ$ , relative to the tetragonal symmetry  $c$  axis. As the temperature is raised,  $H_{\text{eff}}$  decreases and disappears completely at  $T_N(\text{Ru})=180(5)$  K.  $H_{\text{eff}}$  values obtained at 110, 130, 150, and 160 K are 399(3), 358(5), 312(2), and 279(5) kOe. The variation of the normalized  $H_{\text{eff}}(T)/H_{\text{eff}}(0)$  values, as a function of the reduced temperature, is exhibited in Fig. 3. Close to 180 K, due to a distribution of  $T_N$  resulting from inhomogeneity in the local environment of Fe throughout the Ru site, a distribution in  $H_{\text{eff}}$  is assumed and a paramagnetic doublet in the central area of the spectra is observed.

It was shown theoretically<sup>10</sup> for all Fe-doped Y-Ba-Cu-O (as well as  $M-2122$ ) materials, that when Fe reflects the magnetic behavior of Cu(2) sites, the normalized  $H_{\text{eff}}$  values fall on one universal curve, regardless of Fe or oxygen concentration and whether Y is replaced by Pr. The model assumes that the temperature dependence of magnetization of Cu(2) and  $\text{Fe}^{3+}$  as a probe behaves like spin- $\frac{1}{2}$  and spin- $\frac{5}{2}$  systems and that the Fe-Cu exchange is only 26% of the Cu-Cu exchange strength. The dashed line in Fig. 3 is the universal theoretical curve calculated in this way. The deviation of the experimental data from this universal curve is our supporting evidence that the magnetic sextet in Fig. 4 is due to Fe in the Ru site. Moreover, the fact that both the reduced magnetic moment obtained directly from the  $M(H)$  curves for  $R=\text{Eu}$  [Fig. 2(b)] and the data obtained from MS for  $R=\text{Gd}$  lie on the same curve indicates clearly that the Ru-Fe and Ru-Ru exchange strengths are quite similar.

We suggest two scenarios that could lead to the observed phenomena. A central assumption is that Ru in  $RCeRuSCO$  orders magnetically at elevated temperatures, and bulk SC is confined to the  $\text{CuO}_2$  planes. Both sublattices are practically decoupled, and thus the present system is the first magnetic-superconducting system in the HTSC-based materials. Supporting evidence for this interpretation is (1) the bulk SF obtained for  $R=\text{Eu}$  in the SC state, and (2) the overlapping of the two normalized curves exhibited in Fig. 3. The second interpretation invokes an analogy to inhomogeneous materi-

als; e.g., the reason for the two physical phenomena are grains with different oxygen concentrations; part of them are SC and the rest magnetic. Moreover, one may argue that the magnetic anomalies exhibited in Figs. 1 and 2 are due to an  $\text{SrRuO}_3$  impurity phase which is ferromagnetically ordered at 165 K.<sup>11</sup> In order to reconcile these arguments we have prepared pure and Fe-doped  $\text{SrRuO}_3$  samples, and measured their magnetic and MS properties. The measured  $\chi(T)$  curve (at 10 Oe) is a typical one obtained for a ferromagneticlike sample, and in the MS spectra at  $T > 90$  K there is no sign whatsoever of magnetic order, indicating a weak-coupling Fe-Ru. Our measurements are consistent with Ref. 11, and are completely different from the data presented in Figs. 1–4. In addition, our STM topography and spectroscopy measurements, described in the next paragraphs, are not consistent, to say the least, with the mixed granular magnetic-SC picture.

The STM topographic images were measured in the constant current mode, where a feedback circuit controls the tip-sample separation for a given setting of the tunneling current  $I_s$  and tip bias  $V_s$ . These images reveal relatively rough surface morphology, with rms roughness amplitude around 50 Å, and surface features of typically a few hundred Å lateral size. The  $I$ - $V$  curves were acquired while momentarily interrupting the feedback circuit. At each lateral tip position these characteristics were taken with different settings, i.e., with different tip-sample separations.

The principal observation of our STM spectroscopy measurements at 4.2 K is the existence of spectroscopic gaps in the  $I$ - $V$  characteristics, which vary in width and shape along the surface of the samples, yet never vanish. However, the width of the gap at a *specific* lateral tip position is not altered by changing the STM setting, indicating that single electron charging effects, e.g., the Coulomb blockade, do not contribute to the spectroscopic gaps.<sup>12</sup> Furthermore, *all*  $I$ - $V$  curves measured at  $\sim 45$  K (*above*  $T_c$ ) exhibit an Ohmic, gapless behavior for small biases, independent of tip position or STM setting. These findings clearly indicate that all the gaps are of SC origin.

The  $I$ - $V$  characteristics were fit using Dyne's expression<sup>13</sup> for lifetime broadened quasiparticle density of states. Thus, two fitting parameters were used: the SC gap parameter  $\Delta$ , and the lifetime broadening of the quasiparticle eigenstates,  $\Gamma$ . In Fig. 5 we present typical experimental  $I$ - $V$  characteristics at 4.2 K for the  $R$ =Eu and Gd samples, together with fits to Dyne's function (smooth lines). In the inset we plot the normalized differential tunneling conductance, manifesting the superconductor quasiparticle density of states. The zero bias conductance apparent from these curves is  $\sim 13\%$  of the conductance at large bias, which is typical for HTSC.<sup>14,15</sup> The fitting parameters used in the theoretical curves are  $\Delta=9$  and 7.7 meV;  $\Gamma=3.5$  and 2 meV for  $R$ =Eu

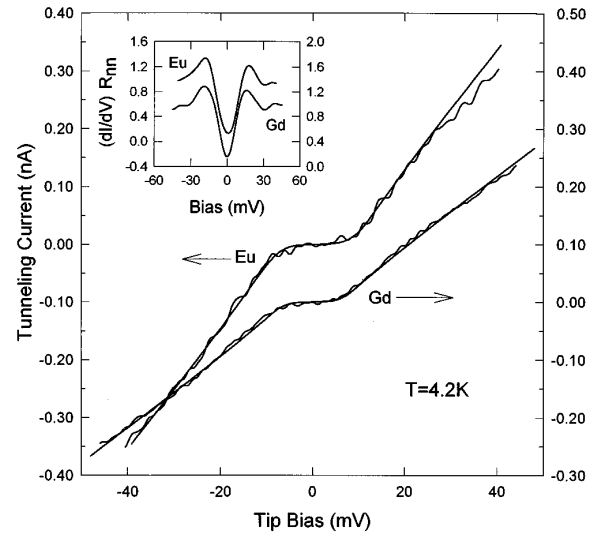


FIG. 5. Tunneling  $I$ - $V$  characteristics at 4.2 K of  $R$ =Eu and Gd samples. The theoretical curves (smooth lines) were calculated using Dyne's function (see text). The inset shows the normalized differential conductance.

and Gd, respectively. It should be emphasized that we have taken  $I$ - $V$  curves in 15 to 20 macroscopically distinct positions, on a dense grid covering a square of side 2000 Å for each position, and *always* found a spectroscopic gap which varied spatially in the range 7–10 meV.<sup>16</sup>

We found that for both  $R$ =Gd and Eu samples, the ratio  $2\Delta/k_B T$  ( $k_B$  is the Boltzmann constant) is in the range 4–7, which is compatible with what was found for Y-Ba-Cu-O.<sup>15</sup> The variation of  $\Delta$  along the sample may be attributed to (a) inhomogeneity of oxygen content over the sample, or (b) the large gap anisotropy expected for HTSC's<sup>14</sup> noting that our samples are polycrystalline, so that tunneling may occur in different crystallographic directions for different tip positions. Note that we did not find sharp spatial transitions between superconducting and normal neighboring surface regions, as might be expected for a granular specimen.<sup>12</sup> Moreover, since we expect SC to be more vulnerable at the surface as compared to the bulk, we can infer SC to the bulk as well. Thus, the STM findings are evidence that our samples are really of single phase, and do not consist of separate superconducting and magnetic grains.

In conclusion, we provide strong evidence that both SC and weak ferromagnetism coexist in  $RCeRuSCO$  and are an intrinsic property of this system. In contrast to other intermetallic magnetic-SC systems, the present materials exhibit magnetic order well above the SC transition ( $T_N/T_c \sim 4$ ). We attribute the magnetic order to the Ru sublattice, whereas SC is confined to the  $\text{CuO}_2$  planes. Both sites are practically decoupled from each other.

This research was supported by the Klachky Foundation for Superconductivity.

<sup>1</sup> *Superconductivity in Ternary Compounds*, edited by M. B. Maple and O. Fisher (Springer-Verlag, Berlin, 1982), Vol. II.

<sup>2</sup> H. Eisake *et al.*, Phys. Rev. B **50**, 647 (1994).

<sup>3</sup> L. Rukang *et al.*, Physica C **176**, 19 (1991).

<sup>4</sup> R. J. Cava *et al.*, Physica C **191**, 237 (1992).

<sup>5</sup> I. Felner *et al.*, Phys. Rev. B **49**, 6903 (1994); **51**, 3120 (1995).

<sup>6</sup> L. Bauernfeind *et al.*, Physica C **254**, 151 (1995).

<sup>7</sup> J. Dzyaloshinsky, J. Phys. Chem. Solids **4**, 241 (1958).

<sup>8</sup> M. Bennahmias *et al.*, Phys. Rev. B **53**, 2773 (1996).

<sup>9</sup> I. Felner *et al.*, Phys. Rev. B **49**, 686 (1994).

<sup>10</sup> I. Nowik *et al.*, Solid State Commun. **74**, 957 (1990).

<sup>11</sup> T. C. Gibb *et al.*, Solid State Chem. **14**, 193 (1975).

<sup>12</sup> E. Bar-Sadeh *et al.*, Phys. Rev. B **52**, 6734 (1995); **53**, 3482 (1996).

<sup>13</sup> R. C. Dynes *et al.*, Phys. Rev. Lett. **41**, 1509 (1978).

<sup>14</sup> J. Kane and K. W. Ng, Phys. Rev. B **53**, 2819 (1996).

<sup>15</sup> H. L. Edwards *et al.*, Phys. Rev. Lett. **69**, 2967 (1992).

<sup>16</sup> O. Millo *et al.*, J. Low Temp. Phys. (to be published).